Modeling and experimental investigations of hydration and physical properties of slag blended cement after long curing period

Mohamad Ali Ahmad

Nantes Université, Ecole Centrale Nantes, CNRS, GeM, UMR 6183 F-44600 Saint-Nazaire, France

RESUME Le laitier de haut fourneau, un sous-produit du processus de fabrication de l'acier, peut être utilisé comme addition minérale dans les ciments composés. Outre la réduction des émissions de CO_2 dans la construction des ouvrages en béton, l'utilisation du laitier dans les matériaux cimentaires peut aussi contribuer à améliorer leurs propriétés de durabilité. Malgré de nombreuses études sur les propriétés d'hydratation des ciments à base de laitier, certains aspects, tels que l'influence du taux de substitution en laitier sur la cinétique d'hydratation, sur et sur les propriétés microstructurales restent encore mal compris. Cette étude est une contribution à une meilleure compréhension de l'hydratation des ciments au laitier à travers la mise en œuvre d'un modèle d'hydratation intégrant à la fois cinétique et réactions chimiques. Les données d'entrée requises sont les paramètres de formulation (rapport eau/liant, taux de substitution du clinker par le laitier) et le type de cure. Le modèle reproduit bien les évolutions du degré d'hydratation, les quantités d'hydrates ainsi que des densités sèches issues de la littérature ou mesurées expérimentalement sur des formulations de pates de ciment contenant respectivement 0%, 30%, 50% et 80% de laitier.

Mots-clefs Ciment à base du laitier de haut fourneau, degré d'hydratation, microstructure, modèle d'hydratation.

I. INTRODUCTION

In a world moving towards more eco-friendly construction, one of the primary challenges in terms of ecological sustainability for the coming decades is to design and produce concretes with less clinker and lower CO_2 emissions while ensuring enhanced durability. Blast Furnace Slag (BFS), a non-metallic mineral by-product of iron production, is widely used in the cement due to its advantageous properties. Studies have explored blending Portland cement with BFS to enhance overall structural performance. Benefits include low heat of hydration (Ben Fraj et al., 2019; Özbay et al., 2016), high chloride resistance (Ben Fraj et al., 2012; Touil et al., 2022), improved compressive strength, and durability (Dhir et al., 1996; Luo et al., 2003).

Knowing that the chemical composition of BFS is closely to that of Ordinary Portland Cement (OPC), its activation typically requires a basic agent, like alkaline (sodium or calcium), sulfatic (gypsum), sulfate-calcium, or sulfate-sodium activation (Cheng et al., 2005; Hadj-sadok et al., 2011; Shi-Ping and Grandet, 1989). This study considers calcium activation using Portlandite $Ca(OH)_2$ generated during clinker hydration.

Despite numerous studies on slag-blended cement hydration processes, understanding the effects of clinker substitution rates by slag on kinetics, mechanisms, and microstructural properties

remains incomplete. The present study aims at filling this gap by involving hydration model that takes both kinetic and chemical aspects into account.

Various approaches for predicting hydration kinetics have been developed in the literature, including analytical and numerical methods. Analytical models, such as those proposed by (Knudsen, 1984; Merzouki et al., 2013), accurately simulate the kinetics evolutions of low slag substitutions but underestimate for higher amounts. Numerical models, like those by (Kolani et al., 2012; Kolani, 2012; Wang, 2021; Wang et al., 2010), use mass and heat balance equations coupled with thermodynamic calculations (Elakneswaran et al., 2016) but referring to the authors themselves, it may overestimate hydration degrees for high slag replacements.

Chemical reaction descriptions have been approached stoichiometrically, but some models lack consideration for hydration evolution over time. Multi-component hydration models, such as (Jennings and Johnson, 1986), HydratiCA (Bullard, 2007), and CEMHYD3D (Bentz and Bentz, 2000), use geochemical approaches with different discretization methods. These models are considered as time consuming.

It is worth noting that this article is a part of my thesis research, which involves developing a comprehensive model starting by exploring the hydration process, continues with an analysis of microstructure, and further investigates transport properties like gas permeability and chloride diffusion. These aspects will be integrated with the chloride fixation isotherm to form a complete and comprehensive coupled model to understand the initiation of corrosion within a blended cement, particularly in a tidal bed, while considering different tidal cycles (Reuge et al., 2023).

In this regard, this study aims at achieving a better comprehension of the long-term characteristics of BFS-blended cement through the development of a hydration model considering both kinetics and chemical reactions with few input data. Through this objective, the study aims to contribute valuable insights into the long-term performance of BFS-blended cement by integrating hydration kinetics, chemical reactions, and physical property estimation. Analytical models are proposed for predicting hydration kinetics, validated and calibrated through experimental results from Thermal Gravimetric Analysis (TGA). TGA is used to estimate the hydration degree of cement paste incorporating various slag rates at different ages. A modified version of the stoichiometric model proposed by (Kolani et al., 2012), allowing to predict the consumed Portlandite content without the passing through a numerical resolution of a system of equations of mass and heat balances is used to describe the chemical reactions during the hydration process. The output data of the model includes hydrated and anhydrous phases and dry densities. The approach is validated experimentally and based on literature findings of different formulations. The proposed model is able to predict the properties of any BFS blended formulations even at long-term.

II. Hydration model

a. Kinetic model:

In the literature (Deboucha et al., 2017; Lang et al., 2019; Stephant et al., 2014), the mean hydration degree (α) of a slag-blended cement is calculated as a weighted average of clinker and slag hydration degrees, denoted as f_c and f_s, respectively, in Equation 1. As already mentioned previously, α is estimated through the TGA method based on prior research conducted in the laboratory.

$$\alpha = f_c \times \alpha_c + f_s \times \alpha_s \quad \text{Equation 1}$$

For predicting the hydration degrees of clinker and slag, the Avrami exponential-type function (Avrami, 1941, 1940, 1939) is chosen due to its suitability for describing nucleation and growth reactions. This model is expressed in Equation 2, where α_i represents clinker or slag, $\alpha_{i,max}$ is the ultimate hydration degree, S_i is a rate constant, and n_i is an exponent combining time dependencies.

$$\alpha_i = \alpha_{i,max} \times [1-\exp(-S_i \times (t)^{ni})] \quad (i = c \text{ for clinker or } s \text{ for slag}) \quad \text{Equation 2}$$

The ultimate hydration of clinker ($\alpha_{c,max}$) is determined using a relationship proposed by (Waller, 1999) (Equation 3).

$$\alpha_{c,max} = 1-\exp(-D \times (W/C)) \quad \text{Equation 3}$$

In parallel, the evolution of $\alpha_{s,max}$ with respect to the substitution rate of clinker by slag is not clearly established in the literature; hence, a linear evolution is proposed. Once the two ultimate hydration degrees are determined, the two parameters S_i and n_i, for both clinker and slag, can be calibrated and are assumed to vary following a linear regression with respect to the slag content as demonstrated in (Ali Ahmad et al., 2024) by minimizing squared deviations between predicted and estimated values of α at different ages from TGA on the various cement paste formulations.

b. Chemical model:

The study utilizes stoichiometric calculations developed by (Kolani et al., 2012; Kolani, 2012) to describe chemical reactions during the hydration of slag-blended cements. The calculations consider two categories of hydrates formed during clinker and slag hydration. The concentrations of hydrated and anhydrous phases are expressed as functions of time, allowing for the determination of mass and volume of these phases. The study decouples kinetics and chemical aspects for simplified analytical resolution, different from the coupled approach by Kolani.

$$m_{i,hydrated} = \alpha_i \times m_{i0} \quad \text{Equation 4}$$

$$m_{i,non\text{-}hydrated} = (1-\alpha_i) \times m_{i0} \quad \text{Equation 5}$$

where $m_{i,0}$ represents the initial mass introduced in the mixture for each component i (clinker or slag). Depending on the chemical composition of cement and slag, the amounts of hydrated oxides are calculated using the following equation:

$$[j]_{hydrated,i} = m_{i,hydrated} \times F_{j,i} / M_j \quad \text{Equation 6}$$

where j represents the different oxides in the anhydrous phases. $[j]_{hydrated,i}$ is the molar concentration (mol/g) of the hydrated oxide j in the initial introduced mass of component m_{i0}; $F_{j,i,}$ and M_j represent the percentage of the oxide j in the binder i, and the molar mass of j (g/mol), respectively. The stoichiometric equations are detailed in Kolani's thesis (Kolani, 2012). For clinker, the hydration results various hydrates such as calcium silicate hydrates (CSH), Portlandite (CH), Ettringite (AFt), and Monosulfoaluminate (AFm). The hydration of slag consumes a part of this produced CH, however this quantity cannot be determined. In this regard, we simplify the estimation of remaining Portlandite ($[CH]_{c,\ remaining}$) by assuming it is proportional to the already estimated Portlandite reported in (Kolani, 2012) and noted as $[CH]_{c,\ formed}$ (t).

$$[CH]_{c,\ remaining}(t) = \lambda \times [CH]_{c,\ formed}(t) \quad \text{Equation 7}$$

The coefficient of proportionality (λ) is determined by comparing available CH levels from TGA and model predictions (Figure 1), resulting in a found value of λ equal to 0.8. A lower λ is expected, indicating that only 20% of Portlandite generated by clinker hydration is assumed to be consumed by slag hydration. This may be due to the potential underestimation of CH formation during clinker hydration, which relies solely on the chemical composition of the clinker. The influence of slag is

considered through the substitution rate, but the complex interactions between clinker and slag will be considered in future studies.

The evolution of slag hydrates, including calcium aluminate silicate hydrates (CASH), Hydrotalcite (HT), Ettringite (Aft), and Hydrogarnet (AH), is also calculated following the stoichiometric equations reported in (Kolani, 2012) and depending on many ratio; where $(A/S)_{sc}$ represents the molar ratio A/S formed by the slag in the presence of clinker. It is estimated by (Richardson, 1999) by the following relationship:

$$(A/S)_{sc} = (1/4.732)\times[\ 1\text{-}0.4277*(C/S)_s] \qquad \textit{Equation 8}$$

Based on the findings of (Adenot, 1992) and (Brouwers, 2004) which are adopted by (Kolani et al., 2012) the following relation is considered: $(C/S)_s = (H/S)_s = 1.14$. Knowing that $(H/S)_s$ is the water demand of the CASH of the slag alone. The knowledge of this parameter allows quantifying the reacted water with the CASH. The quantification of the reacted water with all the hydrates leads to the identification of the free water quantity available at each time, allowing further prediction of the porosity. In the case of BFS-blended cement, the water demand of CASH formed by the hydration of the slag in the presence of the OPC is evaluated by a linear interpolation between the water demand of CSH_c of the OPC and that of $CASH_s$ of the BFS.

$$(H/S)_{sc}(t) = (C/S)_{sc}(t) +1.45\times((C/S)_{sc}(t)- (H/S)_s(t)) \qquad \textit{Equation 9}$$

where the $(C/S)_{sc}$ takes into consideration both hydrates, CSH and CASH, as follows:

$$(C/S)_{sc}(t) = (C/S)_c\times k_c(t)+ (C/S)_s\times k_s(t) \qquad \textit{Equation 10}$$

It is important to clarify that the formation of the CASH requires the presence of a source of calcium. In the studied formulation, the two sources are the $[CH]_{c,\ remaining}$, and $[C]_{hydrated,s}$. It is worth noting that (Kolani et al., 2012; Kolani, 2012) considered these two equations related directly to the remaining quantity of Portlandite and calcium oxide in the slag. However, as the proportions of Portlandite and calcium in hydrated slag are simply identified with time in this study, k_c and k_s are proposed to satisfy the calcium demand of slag hydrates, to consume the necessary calcium, in proportion to the quantities available in each source as follows:

$$k_c\,(t) = [[CH]_{consumed}\,(t)] / [([CH]_{consumed}\,(t)) + [C]_{hydrated,s}\,(t)] \qquad \textit{Equation 11}$$

$$k_s\,(t) = [C]_{hydrated,s}\,(t) / ([CH]_{consumed}\,(t) + [C]_{hydrated,s}\,(t)) \qquad \textit{Equation 12}$$

Finally, the mass and volume of the hydrates are calculated by multiplying the molar content by either the molar mass or the molar volume, respectively, as shown in the following equations:

$$m_{h,i}\,(t) = M_h \times[h]_i\,(t) \qquad \textit{Equation 13}$$

$$V_{h,i}\,(t) = V_{m,h} \times[h]_i\,(t) \qquad \textit{Equation 14}$$

where h, $[h]_i$, M_h, and $V_{m,h}$ are the hydrates, the content of this hydrate h in the component i, the molar mass and the molar volume of the hydrate h respectively. The evolution of the remaining Portlandite with respect to the solid mass available at time t is also taken into consideration, to be compared at a later stage to the results of the TGA measurements. In order to estimate it, the following equation is proposed:

$$\%_m\ CH_{remaining}\,(t) = m\ CH_{remaining}\,(t)/\ [\sum(m_{i,hydrated}\,(t)+m_{i,non\text{-}hydrated}\,(t)\ \text{-}m(rw)_i\,(t))] \qquad \textit{Equation 15}$$

where $m_{rw,i}$ represents the mass of the reacted water of each hydrate of the binder i at time t. It can be calculated from the quantity of the reacted water in moles per mole of hydrate "$n(rw)_h$" in each binder, which can be identified from the chemical formula of the hydrate. Then the sum of the reacted water at time t can be given as follow:

$$\sum m(rw)_i\,(t) = n(rw)_h \times [h]_i\,(t) \times M_{H2O} \quad \textit{Equation 16}$$

where M_{H2O} is the molar mass of water (18 g/mol).

Concerning the dry density, which represents the mass of solid phases corresponding to a given volume, it can also be estimated with the model using the following equation:

$$\varrho_{dry}\,(t) = \sum (m_{h,i}\,(t) + m_{i,non\text{-}hydrated}\,(t)) \,/\, (V_{total}) \quad \textit{Equation 17}$$

For the estimation of the capillary porosity, the calculation of the capillary pores volume is required and given in the following equation:

$$V_{cap\ pores} = \sum (V_{i0} + V_{entrapped\ air}) - (V_{h,i}\,(t) + V_{i,non\text{-}hydrated}\,(t)) \quad \textit{Equation 18}$$

where V_{i0} , $V_{i,non\text{-}hydrated}$, and $V_{entrapped\ air}$ are the initially introduced volume, the volume of the non-hydrated phases of the binder i, and the volume of the entrapped air, respectively.

$$V_{i0} = m_{i0} / \varrho_i \quad \textit{Equation 19}$$

$$V_{i,non\text{-}hydrated}(t) = m_{i,non\text{-}hydrated}\,(t) / \varrho_i \quad \textit{Equation 20}$$

$V_{entrapped\ air}$ is measured experimentally and is found varying around 3.57% of the initially introduced volume V_{i0}. The capillary porosity can then be written as follow:

$$\Phi_{cap}\,(t) = V_{cap\ pores} / (V_{i0} + V_{entrapped\ air}) \quad \textit{Equation 21}$$

The study provides equations for calculating the mass and volume of hydrates, remaining Portlandite, dry density, and capillary porosity over time in slag-blended cement. The model's parameters are derived from experimental data and calibrated to match TGA results.

III. Experimental procedure and characterization methods

a. Materials

The experimental campaign involves studying slag-based cement pastes with different substitution rates by mass of clinker (CEM I 52.5 N SR5 PM-CP2 HTS cement by Lafarge from Le Teil (France), with a density of 3.17 g/cm^3), by BFS (Produced by Ecocem in Dunkerque, France with a density of 2.9 g/cm^3): 0% (P0), 30% (P30), 50% (P50), and 80% (P80). A constant water-to-binder ratio (W/B) of 0.5 is maintained for all formulations, enabling comparisons with a normalized mortar. The four cement paste mixtures were cast into 40*40*160 mm^3 molds according to the standard (NF EN 196-3, 2017). After casting, plastic films were placed over the molds for 24 hours to reduce water evaporation. Following the demolding process, the samples were immersed in water to achieve saturation, hence enhancing the hydration reactions.

b. Thermogravimetric Analysis

TGA allows both the calibration of kinetic model parameters and the validation through the quantification of certain phases such as Portlandite; it is conducted on ground powder having a particle size lower than 0.4 µm in a nitrogen atmosphere. The apparatus used is a TG/DSC-1, STARe Software 9.30, Mettler-Toledo, with a balanced accuracy of 0.1 µg. All the samples are decomposed during a dynamic heating ramp ranging between 20 and 1025 °C at a rate of 5°C/min. The powder was not dried prior to TG tests to avoid hydrate instability (Baroghel-Bouny, 2004; Deboucha et al., 2017; Taylor, 1997).

The decomposition of cement hydrates is observed during TGA by decreased endothermic peaks on the derivative TGA. The cement hydrate decomposition may be divided into three stages:

- between 25 and 400 °C:
  - Removal of the evaporable water (25 to 105°C)
  - dehydration reaction of CSH and CASH noted as “Ldh” (105 to 400 °C)

- between 400 and 600 °C: dehydroxylation of Portlandite, noted as "Ldx"
- between 600 and 800 °C: decarbonation of $CaCO_3$, noted as "Ldc"

Furthermore, the temperature ranges of each phase vary from one author to another, with low differences depending on the machine used (Bhatty, 1986; Deboucha et al., 2017; Monteagudo et al., 2014). Based on TG results, a method developed by (Monteagudo et al., 2014) and recently improved by (Deboucha et al., 2017) is used to estimate the mean value of hydration degree. Such a method is based on a measurement of the chemically bound water of mineral additions blended into cement paste at time t "$W_B(t)$" with respect to the ultimate chemically bound water ($W_{B\infty}$) and mass of equivalent binder (L_{eq}) in the sample as described in Equation 22.

$$\alpha = (W_B(t)) / (W_{B\infty} \times L_{eq}) \quad \textit{Equation 22}$$

$W_{B\infty}$ (g) is considered equal to 0.24, as assumed by several authors (Deboucha et al., 2017; Monteagudo et al., 2014). The mass of equivalent binder L_{eq} (g) is calculated as Equation 23 by introducing the activity coefficient K = 0.9 for the studied slag according to EN NF 206-1 and NF P18-305 standards (EN NF 206-1, 2004; NF P18-305, 1996).

$$L_{eq} = m_C + K \times m_S \quad \textit{Equation 23}$$

The calculation methods for m_C and m_S are given in Equation 24 & Equation 25.

$$m_C = [m_{sample} - m_B \times (f_S + W/B)] / [(1 + LOI_C)] \quad \textit{Equation 24}$$

$$m_S = [m_{sample} - m_B \times ((1 - f_S) + W/B))] / [(1 + LOI_S)] \quad \textit{Equation 25}$$

where m_B, fs, W/B, and LOI represent: the binder mass (g), the replacement rate of OPC by slag, the water/binder ratio, and the loss on ignition, respectively. W_B can be calculated as follows:

$$W_B(t) = Ld_h + Ld_x + 0.41(Ld_c - Ldc_S) - (m_C \times LOI_{CC} + m_S \times LOI_{SC}) + m_d \quad \textit{Equation 26}$$

where Ldc_S, LOI_{ic}, and m_d are the relative mass losses during the decarbonation phase (between 600 and 1000°C) of the anhydrous material, the loss on ignition of anhydrous powder mass, and the device's drift, which is the mass variation of an empty crucible (g) subjected to a high temperature, respectively. The constant "0.41" represents the conversion factor, which allows assuming the bound water is derived from carbonated Portlandite (Deboucha et al., 2017).

The determination of the experimental content of Portlandite at a given period of time t with respect to the dry mass is also possible. It is given by following the equation, based on TGA:

$$\%Ca(OH)_2(t) = (Ld_x \times M_{Ca(OH)2}) / (m_{600°C} \times M_{H2O}) \quad \textit{Equation 27}$$

c. Dry density and porosity

The dry density and the water porosity are assessed following the procedure outlined in the French standard (AFNOR, 2022) and calculated using the formula:

$$\Phi = (m_{sat} - m_{dry}) / (m_{sat} - m_{hydro}) \quad \textit{Equation 28}$$

$$\varrho_{dry} = (m_{dry}) / (m_{sat} - m_{hydro}) \quad \textit{Equation 29}$$

where Φ, m_{sat}, m_{dry}, m_{hydro} and ϱ_{dry} are the porosity, sample saturated mass, the dry mass measured after drying at 105°C, the hydrostatic mass and the dry density respectively.

IV. Results and discussion

a. Hydration kinetics

In general, the hydration kinetics of BFS is slower than that of OPC. Figure 1 illustrates the hydration kinetics for four cement paste formulations (P0, P30, P50, and P80) over 960 days. The initial dilution effect of slag is evident, with lower hydration degrees at 7 days (0.67, 0.54, 0.53, and

0.38 for P0, P30, P50, and P80, respectively). Despite increased values between 7 and 360 days (0.91, 0.83, 0.73, and 0.49); the dilution effect persists, as indicated by the stable CH amount.

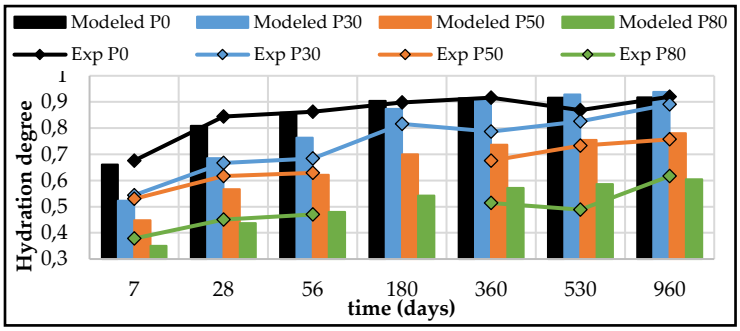

Figure 1. ***Hydration degree based on TGA used to calibrate the model***

At 530 days, hydration degrees for slag-blended cement pastes, especially P30, notably increase, becoming comparable to P0. The hydration degrees at 530 days are 0.87, 0.89, 0.76, and 0.62 for P0, P30, P50, and P80, respectively. Beyond this point, P0 and P30 exhibit similar hydration degrees, while P50 and P80 remain lower. After 960 days, the hydration degrees for P0, P50, and P80 are 0.92, 0.90, 0.73, and 0.53, respectively. The decrease reported for P80 between 530 and 960 days may be due to measurement uncertainty, though it suggests stabilization. Hydration kinetics reveal that P0 reaches a hydration degree of 0.86 at 90 days, slowly increasing to 0.9 at 180 days before stabilizing. Slag-blended cement shows a steep increase until 90 days, with a slower rate after 90 days, indicating prolonged hydration up to 960 days. The kinetics shift, highlighting increased slag hydration over time.

Calibrating parameters, reported in details in (Ali Ahmad et al., 2024), for clinker and slag hydration kinetics are achieved using experimental results. For clinker, coefficients a_{nc}, b_{nc}, a_{sc}, and b_{sc} are determined from P0 results. The dilution effect is consistent with increased accessibility of water for clinker hydration with higher BFS content. Parameters n_c, S_c, and $\alpha_{c,max}$ are calibrated using P0, while coefficients a_{ns}, b_{ns}, a_{ss}, b_{ss}, $a_{\alpha s}$, and $b_{\alpha s}$ are calibrated from P30, P50, and P80 results. These coefficients show significant variations with slag content, representing complex physico-chemical mechanisms.

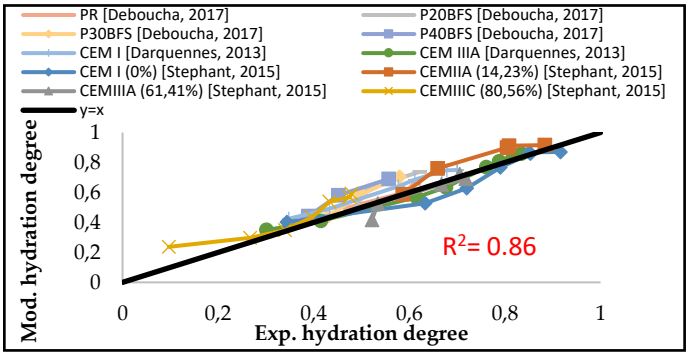

Figure 2. ***Model validation based on experimental hydration degrees from literature***

In order to validate the hydration kinetic models proposed in this study, a comparison between experimental data reported from the literature and the predicted ones was made and presented in

Figure 2. The various tested mixes in terms of W/B ratio, curing type and duration, binder compositions, and BFS content, are recorded in **TABLE 1**.

TABLE 1. Parameters used in the literature

Reference	W/B	Cure time (days)	Cure type	BFS content (%)
(Stephant et al., 2014)	0.41 and 0.43	1; 3; 7; 28; 180; 360; 730	Water	0; 14.26; 61.41; 80.56
(Darquennes et al., 2013)	0.45	0.5; 2; 5; 21; 42; 215; 420; 1970; 4090	Air	0; 42
(Deboucha et al., 2017)	0.35	7; 28; 90	Air	0; 20; 30; 40

b. Hydrates content and model's validation

In the initial phase, the study focuses on the evolution of CH in various cement paste mixes, as depicted in Figure 3. The measurements based on TGA results, reveal interesting patterns.

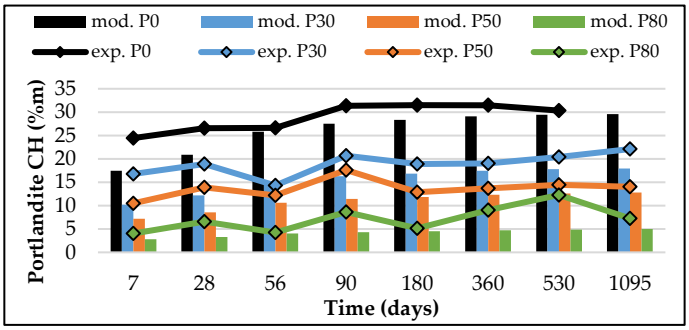

Figure 3. ***Experimental and modeled CH content used to calibrate (P80) and validate the model (P30 & P50)***

For the P0 formulation, CH content increases from 23.40% to 30.15% at 7, 56, and 90 days, stabilizing thereafter. Typically, completely hydrated OPC generates around 20 to 25 wt.% $Ca(OH)_2$. However, this weight percentage is relative to the binder mass. The introduction of slag results in a drop in generated Portlandite due to the early-age slag dilution effect, as observed in P30, P50, and P80 formulations (Figure 3). Available Portlandite content increases for all formulations up to around 90 days, aligning with hydration degree evolution. The stabilization of available CH over time suggests a constant ratio between CH formed by clinker hydration and the remaining ratio after slag hydration, supporting the proportionality assumption in Equation 7, where the coefficient of proportionality (λ) is calibrated using P80 formulation. It is then validated against P30 and P50 formulations, along with 86 literature results with BFS content ranging from 0 to 80.56%, (Ali Ahmad et al., 2024). However, it is acknowledged that Equation 7 may not perfectly capture short-term slag-based cement hydration, as some studies report CH content increasing and then decreasing at early ages, a trend not precisely described in the model. Despite this, it effectively reproduces the overall trend of experimentally measured Portlandite evolution, particularly at long-term intervals.

Additionally, given its ability to calculate the amount of both hydrated and anhydrous phases, the hydration model can estimate the dry density as described in Equation 17. It is important to highlight that the accurate prediction of dry densities, as demonstrated in **Figure 4**, serves as an additional validation of the calculations of anhydrous phases and hydrates, beyond just Portlandite. These include hydrates like CASH or Aft, which might pose challenges when it comes to experimental quantification. **Figure 4** highlights that increasing slag content leads to a decrease in dry density due to higher amounts of anhydrous phases. Such result is expected since they are consistent with lower hydration degrees previously shown in Figure 1, leading to a higher

anhydrous phases. The dry density of P0 formulation increases significantly until 28 days and then tends to stabilize while a slower but progressive increase is observed for cement pastes formulated with slag. This is attributed to the formation of new hydrates able to fill the existent pores, leading to a decrease in the void ratio and then an enhancement in density, as reported in (Song et al., 2000).

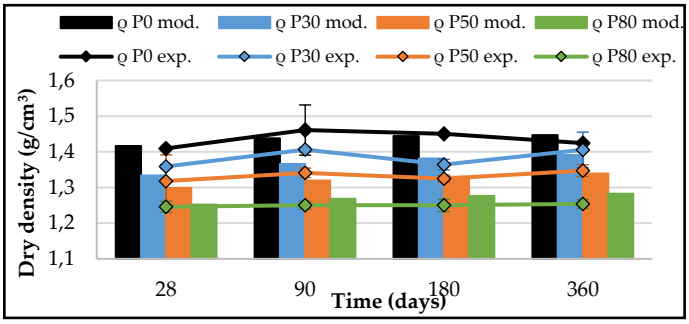

Figure 4. ***Comparison between experimental and modeled dry density (model validation)***

Finally, concerning the porosity, the prediction of capillary porosity ((Equation 21) is discussed in relation to hydration, emphasizing the challenge of accurately estimating total porosity due to the influence of slag on intra-hydrate porosity of CSH and CASH. Contradictory information about CASH porosity in the literature leads to the consideration of only capillary porosity in this model, in this regard, deeper investigations taking into account the effect of slag on the intra-hydrates porosity are being conducted and will be considered during the oral presentation and published in further works.

V. Conclusion

This study enhances our understanding of BFS-blended cement hydration mechanisms by developing a comprehensive model that considers both kinetics and chemical reactions. The proposed approach requires minimal parameters associated with formulation characteristics. The key findings include the description of hydration kinetics using adapted Avrami's exponential models, chemical reactions using a modified version of Kolani's stoichiometric model, and successful calibration based on experimental data from various slag ratios.

The model reproduces essential output data, such as hydration degree evolution, hydrated phases, and dry densities. Further investigation is needed to understand the impact of different slag ratios on the porous structure of CSH and CASH. Future studies may explore combining this model with thermodynamic approaches for a detailed understanding of slag hydration activation and concrete early age cracking risk quantification.

VI. Acknowledgments

I would like to explicitly thank the Association Universitaire de Génie Civil (AUGC) for their support of my mobility, as well as the Unité de Technologie et de Recherche en Ingénierie Verte (UTR INGVER) of the GeM laboratory.

VII. REFERENCES

Adenot, F., 1992. Durabilite du beton : caracterisation et modelisation des processus physiques et chimiques de degradation du ciment (thesis). http://www.theses.fr. Orléans.

AFNOR, 2022. Essai Pour Béton Durci—Essai de Porosité et de Masse Volumique—NF P18-459.

Ali Ahmad, M., Ranaivomanana, H., Bonnet, S., Buttin, P., L'Hostis, V., 2024. Contribution to a better understanding of long-term hydration, structuration and mechanical properties of slag based cementitious materials: Experimental and modeling approaches. Construction and Building Materials 411, 134664. https://doi.org/10.1016/j.conbuildmat.2023.134664
Avrami, M., 1941. Granulation, Phase Change, and Microstructure Kinetics of Phase Change. III. The Journal of Chemical Physics 9, 177–184. https://doi.org/10.1063/1.1750872
Avrami, M., 1940. Kinetics of Phase Change. II Transformation-Time Relations for Random Distribution of Nuclei. The Journal of Chemical Physics 8, 212–224. https://doi.org/10.1063/1.1750631
Avrami, M., 1939. Kinetics of phase change. I General theory. The Journal of chemical physics 7, 1103–1112.
Baroghel-Bouny, V., 2004. Which toolkit for durability evaluation as regards chloride ingress into concrete? Part II: Development of a performance approach based on durability indicators and monitoring parameters, in: Third International RILEM Workshop on Testing and Modeling Chloride Ingress into Concrete. pp. 137–163.
Ben Fraj, A., Bonnet, S., Khelidj, A., 2012. New approach for coupled chloride/moisture transport in non-saturated concrete with and without slag. Construction and Building Materials 35, 761–771. https://doi.org/10.1016/j.conbuildmat.2012.04.106
Ben Fraj, A., Bonnet, S., Leklou, N., Khelidj, A., 2019. Investigating the early-age diffusion of chloride ions in hardening slag-blended mortars on the light of their hydration progress. Construction and Building Materials 225, 485–495. https://doi.org/10.1016/j.conbuildmat.2019.07.185
Bentz, D.P., Bentz, D.P., 2000. CEMHYD3D: A three-dimensional cement hydration and microstructure development modelling package. Version 2.0. US Department of Commerce, National Institute of Standards and Technology.
Bhatty, J.I., 1986. Hydration versus strength in a portland cement developed from domestic mineral wastes — a comparative study. Thermochimica Acta 106, 93–103. https://doi.org/10.1016/0040-6031(86)85120-6
Brouwers, H.J.H., 2004. The work of Powers and Brownyard revisited: Part 1. Cement and Concrete Research 34, 1697–1716. https://doi.org/10.1016/j.cemconres.2004.05.031
Bullard, J.W., 2007. A three-dimensional microstructural model of reactions and transport in aqueous mineral systems. Modelling and Simulation in Materials Science and Engineering 15, 711.
Cheng, A., Huang, R., Wu, J.-K., Chen, C.-H., 2005. Influence of GGBS on durability and corrosion behavior of reinforced concrete. Materials Chemistry and Physics 93, 404–411. https://doi.org/10.1016/j.matchemphys.2005.03.043
Darquennes, A., Espion, B., Staquet, S., 2013. How to assess the hydration of slag cement concretes? Construction and Building Materials 40, 1012–1020. https://doi.org/10.1016/j.conbuildmat.2012.09.087
Deboucha, W., Leklou, N., Khelidj, A., Oudjit, M.N., 2017. Hydration development of mineral additives blended cement using thermogravimetric analysis (TGA): Methodology of calculating the degree of hydration. Construction and Building Materials 146, 687–701. https://doi.org/10.1016/j.conbuildmat.2017.04.132
Dhir, R.K., El-Mohr, M.A.K., Dyer, T.D., 1996. Chloride binding in GGBS concrete. Cement and Concrete Research 26, 1767–1773.
Elakneswaran, Y., Owaki, E., Miyahara, S., Ogino, M., Maruya, T., Nawa, T., 2016. Hydration study of slag-blended cement based on thermodynamic considerations. Construction and Building Materials 124, 615–625. https://doi.org/10.1016/j.conbuildmat.2016.07.138
EN NF 206-1, 2004. Concrete - Part 1: Specification, performance, production and conformity.
Hadj-sadok, A., Kenai, S., Courard, L., Darimont, A., 2011. Microstructure and durability of mortars modified with medium active blast furnace slag. Construction and Building Materials 25, 1018–1025. https://doi.org/10.1016/j.conbuildmat.2010.06.077
Jennings, H.M., Johnson, S.K., 1986. Simulation of microstructure development during the hydration of a cement compound. Journal of the American Ceramic Society 69, 790–795.
Knudsen, T., 1984. The dispersion model for hydration of Portland cement I. General concepts. Cement and concrete research 14, 622–630.
Kolani, B., Buffo-Lacarrière, L., Sellier, A., Escadeillas, G., Boutillon, L., Linger, L., 2012. Hydration of slag-blended cements. Cement and concrete composites 34, 1009–1018.
Kolani, L., Batian ;. Escadeillas, Gilles ;. Sellier, Alain ;. Lacarrière, 2012. Comportement au jeune âge des structures en béton armé à base de liants composés aux laitiers (PhD Thesis).
Lang, W., Liping, Z., Jian, T., 2019. Hydration Kinetics Model of Slag-blended Cement System. IOP Conference Series: Earth and Environmental Science 242, 062074. https://doi.org/10.1088/1755-1315/242/6/062074
Luo, R., Cai, Y., Wang, C., Huang, X., 2003. Study of chloride binding and diffusion in GGBS concrete. Cement and Concrete Research 33, 1–7.
Merzouki, T., Bouasker, M., Khalifa, N.E.H., Mounanga, P., 2013. Contribution to the modeling of hydration and chemical shrinkage of slag-blended cement at early age. Construction and Building Materials 44, 368–380. https://doi.org/10.1016/j.conbuildmat.2013.02.022
Monteagudo, S.M., Moragues, A., Gálvez, J.C., Casati, M.J., Reyes, E., 2014. The degree of hydration assessment of blended cement pastes by differential thermal and thermogravimetric analysis. Morphological evolution of the solid phases. Thermochimica Acta 592, 37–51. https://doi.org/10.1016/j.tca.2014.08.008
NF EN 196-3, 2017. Méthodes d'essai des ciments — Partie 3 : Détermination du temps de prise et de la stabilité.
NF P18-305, 1996. Ready-mixed concrete.
Özbay, E., Erdemir, M., Durmuş, H.İ., 2016. Utilization and efficiency of ground granulated blast furnace slag on concrete properties – A review. Construction and Building Materials 105, 423–434. https://doi.org/10.1016/j.conbuildmat.2015.12.153
Reuge, N., Bignonnet, F., Bonnet, S., 2023. Sensitivity analysis of a physicochemical model of chloride ingress into real concrete structures subjected to long-term exposure to tidal cycles. Applied Ocean Research 138, 103622. https://doi.org/10.1016/j.apor.2023.103622
Richardson, I.G., 1999. The nature of C-S-H in hardened cements. Cement and Concrete Research 29, 1131–1147. https://doi.org/10.1016/S0008-8846(99)00168-4
Shi-Ping, J., Grandet, J., 1989. Evolution comparee des porosites des mortiers de ciment au laitier et des mortiers de ciment portland. Cement and Concrete Research 19, 487–496. https://doi.org/10.1016/0008-8846(89)90037-9
Song, S., Sohn, D., Jennings, H., Mason, T., 2000. Hydration of Alkali-Activated Ground Granulated Blast Furnace Slag. Journal of Materials Science 35, 249–257. https://doi.org/10.1023/A:1004742027117
Stephant, S., Chomat, L., Nonat, A., Charpentier, T., 2014. Study of the hydration of cement with high slag content. Presented at the 34th annual cement and concrete science conference.

Taylor, H.F.W., 1997. Cement chemistry, 2nd edition.
Touil, B., Ghomari, F., Khelidj, A., Bonnet, S., Amiri, O., 2022. Durability assessment of the oldest concrete structure in the Mediterranean coastline: The Ghazaouet harbour. Marine Structures 81, 103121. https://doi.org/10.1016/j.marstruc.2021.103121
Waller, V., 1999. Relations entre composition des betons, exothermie en cours de prise et resistance en compression (PhD Thesis).
Wang, X.-Y., 2021. Analysis of hydration kinetics and strength progress in cement–slag binary composites. Journal of Building Engineering 35, 101810.
Wang, X.-Y., Lee, H.-S., Park, K.-B., Kim, J.-J., Golden, J.S., 2010. A multi-phase kinetic model to simulate hydration of slag–cement blends. Cement and Concrete Composites 32, 468–477. https://doi.org/10.1016/j.cemconcomp.2010.03.006